DOI: 10.5604/01.3001.0014.7194

Volume 103 • Issue 2 • December 2020

Journal of Achievements in Materials and Manufacturing Engineering

International Scientific Journal published monthly by the World Academy of Materials and Manufacturing Engineering

Characterisation of Mg-Zn-Ca-Y powders manufactured by mechanical milling

S. Lesz [a,*], T. Tański [a], B. Hrapkowicz [a], M. Karolus [b], J. Popis [a], K. Wiechniak [a]

[a] Department of Engineering Materials and Biomaterials, Silesian University of Technology, ul. Konarskiego 18a, 44-100 Gliwice, Poland

[b] Institute of Materials Engineering, University of Silesia, ul. 75 Pułku Piechoty 1a, 41-500, Chorzów, Poland

* Corresponding e-mail address: sabina.lesz@polsl.pl

ORCID identifier: https://orcid.org/0000-0002-2703-2059

ABSTRACT

Purpose: This paper explains mechanical synthesis which uses powders or material chunks in order to obtain phases and alloys. It is based on an example of magnesium powders with various additives, such as zinc, calcium and yttrium.

Design/methodology/approach: The following experimental techniques were used: X-ray diffraction (XRD) method, scanning electron microscopy (SEM), determining particle size distributions with laser measuring, Vickers microhardness.

Findings: The particle-size of a powder and microhardness value depend on the milling time.

Research limitations/implications: Magnesium gained its largest application area by creating alloys in combination with other elements. Magnesium alloys used in various industry contain various elements e.g. rare-earth elements (REE). Magnesium alloys are generally made by casting processes. Consequently, the search for new methods of obtaining materials such as mechanical alloying (MA) offers new opportunities. The MA allows for the production of materials with completely new physico-chemical properties.

Originality/value: Thanks to powder engineering it is possible to manufacture materials with specific chemical composition. These materials are characterized by very high purity, specified porosity, fine-grain structure, complicated designs. These are impossible to obtain with traditional methods. Moreover it is possible to refine the process even further minimalizing the need for finishing or machining, making the material losses very small or negligible. Furthermore material manufactured in such a way can be thermally or chemically processed without any problems.

Keywords: Mg-based alloys, Scanning Electron Microscopy, X-ray diffraction analysis, Mechanical alloying

Reference to this paper should be given in the following way:

S. Lesz, T. Tański, B. Hrapkowicz, M. Karolus, J. Popis, K. Wiechniak, Characterisation of Mg-Zn-Ca-Y powders manufactured by mechanical milling, Journal of Achievements in Materials and Manufacturing Engineering 103/2 (2020) 49-59.

DOI: https://doi.org/10.5604/01.3001.0014.7194

MATERIALS

1. Introduction

Magnesium alloys are widely known in various fields of industry, due to their small weight, good corrosion resistance and excellent properties. This attracts considerable interest for many potential applications such as automotive, aircraft and electronics [1-6]. Presently, however they have relatively low strength, thus remaining rather limited as compared to other alloys, such as aluminium ones. Due to that fact many materials are being investigated as alloying elements for magnesium alloys.

Considerable time and research has been spent into developing magnesium alloys which are alloyed with rare-earth elements, resulting in high-strength [1-5]. They have been made using a vast array of techniques, such as precipitation hardening and grain refinement strengthening to name a few. It is possible to develop materials without rare-earth elements (REE). Yet to this day Mg-RE alloys seem to be the most promising alloys among others [7-11].

This paper will focus on a particular REE – yttrium, it is a silvery-metallic transition metal and is chemically similar to lanthanides. Although its compounds may cause lung disease its biological role is nonexistent. It is interesting due to its strengthening properties, mainly in aluminium and magnesium alloys. It generally improves workability and high temperature oxidation resistance is attractive.

Due to very high solubility of yttrium in magnesium, this REE is one of the most extensively used. Moreover Y additions have a positive effect on the microstructures and mechanical properties. The effect on this microstructures is primarily due to yttrium behaving as an element facilitating the α-Mg nucleation, hence refining the grain. With the addition of yttrium to Mg-Zn alloys further influences all the properties of the alloy [12]. Adding too much will have the effect adverse to the planned one, being detrimental at some point, coarsening the grain and weakening the mechanical properties instead of increasing them. This effect can be reversed by adding more suitable alloying elements, which would form additional intermetallic phases.

Considering the influence of possible alloying elements on the parameters such as biocompatibility, biode-gradability, hydrogen evolution and corrosion-resistant properties. Qu et al. [13] have taken on the development of novel magnesium-based biomaterial with zinc, calcium and yttrium additions. Magnesium alloys with zinc and calcium used presently are known for their excellent mechanical properties. Moreover those additives tend to improve the corrosion resistance. Many research results confirm the beneficial effect of the rare earth elements (such as yttrium, even small addition ~1 at.%) on corrosion resistance and strength.

In theory magnesium based alloys with yttrium and calcium addition can be characterized by better corrosion resistance after the implantation due to the formation of a stable and less reactive hydrogen layer on their surface. Previous research of Qu et al. [13] have proven that in order for the biomaterial to have an acceptable biocompatibility, the calcium content cannot exceed 1 at. %, and zinc 5 at.%. Till now it has not been researched what is the maximum content acceptable of yttrium, in biomedical alloys. It is known however, its excessive concentration provokes an increase in eosinocytes, weight loss and eosinophilic infiltrate in the submucosa.

Despite those flaws, the beneficial effect of yttrium and other REE on the magnesium based alloys was proven to have a positive influence on biomaterials, but only small amounts were accepted [2-4,7-9,11-15].

The Mg-Zn-Ca-Y (Mg-96.5, Zn-2.0, Ca-0.5, Y-1.0 wt.%) alloy was the main focal point of the Qu's et al. [13], was characterized by good corrosion parameters, high biocompatibility in both humans blood and in the experimental rabbits bodies. The haemolysis results and the kidney and liver tissues observations have proven the results of other group scientists researching the biomedical magnesium-based alloys and proofs that they are a real alternative for commonly used materials.

After comparing the results to Gu's and others research [16] it was noted that the haemolysis and tissues inflammation had significantly decreased, as compared to pure magnesium implants and various binary alloys. Qu's et al. [13] has verified that corrosion is the most critical issue, as it is uncontrollable for crystalline alloys and may cause a sharp decrease in the mechanical properties. Among the proposed methods for corrosion resistance, improvements were implant surface modification and alloy amorphization [2,13,17].

The amorphization may be obtained by changing the alloy manufacturing method or by chemical composition modification [18,19]. However there is an alternative method to classically used metallurgy which is powder engineering (PE).

Thanks to recent developments in the powder engineering, these manufactured materials meet both service and durability requirements due to higher densities and strengths. The most advanced manufacturing solution available come up. This method uses metal, non-metal or alloy powders as a base. The powder process is classified among many methods used in the manufacture of nanocomposites (e.g. ceramic), in which compression, rolling, and extrusion are used as the processing method. In order to enhance their properties, materials can be heat treated, either by induction or conventionally. Subsequently,

these powders can be prepared for pouring into moulds or dies, and compacted under pressure. Depending on their process conditions, sintered materials can have properties similar to those after heat treatment, yet with lower cost and more dimensional stability. The variety of metals and alloys, which can be extruded is limitless, as long as the temperatures and pressures involved do not exceed the capabilities of the die [20,21].

One of the methods of powder manufacturing is mechanical synthesis, known as well as mechanical alloying. This method is used for alloy amorphization, but as well as base material milling and to change the order of the intermetallic phases microstructure [22,23].

By modifying the chemical composition Wang and other [24] have researched the effect of yttrium on Mg-Zn-Ca alloy. Mg-Zn-Ca-Y alloys with nominal compositions of 68 at.% Mg, 25-28 at.% Zn, 4 at.% Ca, and 1-3 at.% Y were prepared by melting the mixture of pure magnesium, Zn (99.9 wt.%) and industrial Mg-Ca (Mg-70, Ca-30 wt.%), Mg-Y (Mg-75.3, Y-25.7 wt.%) alloys. The structure was mainly composed of the α-Mg and $Ca_2Mg_6Zn_3$, MgZn phases. After adding Y, the $Mg_{12}YZn$ phase appeared which is characterised by long period stacked order (LPSO) of the crystalline structure. The appearance of the structure is a characteristic trait of the Mg-Zn-RE alloys [14].

Hence it is justified to manufacture Mg-based powders, assessing their properties, which is the aim of this work.

However, magnesium alloys are generally made by casting processes. As an alternative method of producing metallic materials powder engineering can be used [17]. The main issue is that rare-earth elements exhibit a very high melting temperature, thus making the process both difficult and lengthy which obviously results in higher costs.

Powder process is a process which stands out among the more traditional methods such as casting, rolling, machining, extrusion and forging [5,25-30]. This is a consequence of the traditional methods usually being characterized by the secondary and intermetallic phases appearing along the grain boundary [25,26]. This has a negative effect on the alloy due to the variation in the thermal decomposition of different phases [27]. As the powder process is able to fabricate metallic alloys near net shape, avoiding the abovementioned problems, it can be characterized as very fast production method as well as being high-precision and economical [25].

Mechanical alloying (MA) is the process of milling a substance in a solid state to obtain a powder [23,31-34]. The input material consists of pure elements in appropriately selected proportions or alloys that are subjected to the milling process in high-energy mills. The outcome of this process is the formation of particles of similar size, new chemical compounds and the fragmentation of the structure. Due to the cyclic deformations, i.e. welding, crushing and re-welding, the grain size is reduced and new grain boundaries are created. The structure of the material is not stable and as such the alloy may exist as a solid solution, intermetallic phase, a mixture of components or amorphous material [32].

When both powders are plastic and they collide with the balls and the walls of the container and deformation takes place. As a result the grains overlap to form a very developed lamellar structure. On the other hand when one powder is plastic and the other is brittle, the mechanical alloying process leads to a homogeneous distribution of brittle particles in a plastic matrix. During the process cracking and forceful milling of the brittle powder as well as deformation and cracking of the plastic powder take a place [22,33,34].

Five main steps of MA can be distinguish, which are as follows:

- initial – there is a partial deformation of the powder, the development of thin layers with a thickness of 1÷2 of the diameter of the starting powder particles, and different size and hardness of the particles;
- agglomeration of particles – particles under the influence of obtained energy combine into clusters of the so-called agglomerates and the hardness of the ground powder increases under the effect of strain hardening;
- formation of equiaxial particles – with regular, symmetrical and repetitive shapes, the milling of powder particles on the balls and walls of the bowl takes place;
- formation of unequal particles – with irregular shapes, agglomerates of chaotic structures are formed during the joining of equiaxial particles;
- final – particle size distribution is regular and the hardness is saturated, the phase composition of particles changes [22].

In the process of MA, the diffusion rate increases as the process increases the number of defects. The contact area increases during the process by the formation of increasingly thinner layers of ingredients. The parameters of mechanical synthesis on which the strength, physical and chemical properties depend are [22,32]: type of mill, degree of filling the container, size and material of milling media, ratio of milling media mass to powder mass, milling temperature and atmosphere.

2. Experiments

The samples used for this research were obtained by mechanical alloying using a Dual High-Energy Ball Mill – SPEX 8000D Mixer/Mill with 1475 rpm resulting in

875 cycles/minute. The powder mixtures for the mill were prepared beforehand from high purity (≥ 99.99%) magnesium, zinc, calcium and yttrium elements provided by Alfa Aesar. Two sets of powders were prepared. The chemical composition (at.% and wt.%) and designation samples were presented in Table 1. The total mass of elements used for the tests was 10 g, as it was the maximum volume capacity of stainless steel containers used in the process. The elements were weighted and then enclosed under a protective argon atmosphere.

Both samples were prepared with a ball-to-powder ratio equal to 10:1, with different ball diameters. The Mg-2at.%Zn powders was prepared with 10 mm, and Mg-27at.%Zn with 5 mm ball diameter. Both powder mixtures were milled for 3, 5 and 8 hours, respectively. Each milling cycle consisted of a 1 hour milling time and a 30 minute cooldown period in order to avoid friction welding.

The examination steps which followed consisted of a scanning electron microscopy (SEM) equipped with an energy-dispersive spectrometer (EDS), performed on Zeiss SUPRA 35 microscope and Trident XM4 EDS with 20 kV of accelerating voltage. The EDS analysis was carried out on the surface of a metallographic specimen for Mg-2at.%Zn and Mg-27at.%Zn samples after 3, 5 and 8 hours of milling time. Accuracy of the main and major element in wt.% are 2 % and 4%, respectively and for a minor and trace elements are in a range of 10-20 % and 50-100%, respectively.

The microhardness of the powder samples were analysed on a Future-Tech FM700 Vickers hardness tester with a 15 seconds dwell time and 50 grams of force on samples prepared in resin. These were ground and polished before testing.

Particle size distributions with laser measuring using a Fritsch Analyssette 22 MicroTec+ in a wet chamber filled with ethyl alcohol was determined. The alcohol was used to diminish both the oxygen influence on the sample and to avoid an unwanted chemical reaction with the water medium.

The X-ray diffraction (XRD) measurements were performed by using the PANalytical Empyrean Diffractometer with Cu-Kα radiation (λ $K_{\alpha 1}$ = 1.5418Å) and a PIXcell detector. The phase analysis was conducted using the HighScore Plus PANalytical software integrated with the ICDD crystallographic data base PDF4+ 2018. Structure analysis and crystallite size determination of synthesed phase were performed by Rietveld analyses (High Score Plus software).

3. Results

3.1. X-Ray diffraction

Figure 1 shows XRD patterns of Mg-2at.%Zn (Fig. 1a) and Mg-27at.%Zn (Fig. 1b) samples after different milling time (3, 5 and 8 hours). The results of structure analysis of both samples are presented in Tables 2 and 3.

Table 1.
Chemical composition (atomic and weight %) of the investigated samples

Sample name	wt.%				at.%			
	Mg	Zn	Ca	Y	Mg	Zn	Ca	Y
Mg-2at.%Zn	90.7	5.1	0.8	3.4	96.5	2.0	0.5	1
Mg-27at.%Zn	45.1	48.1	4.4	2.4	68.0	27.0	4.0	1

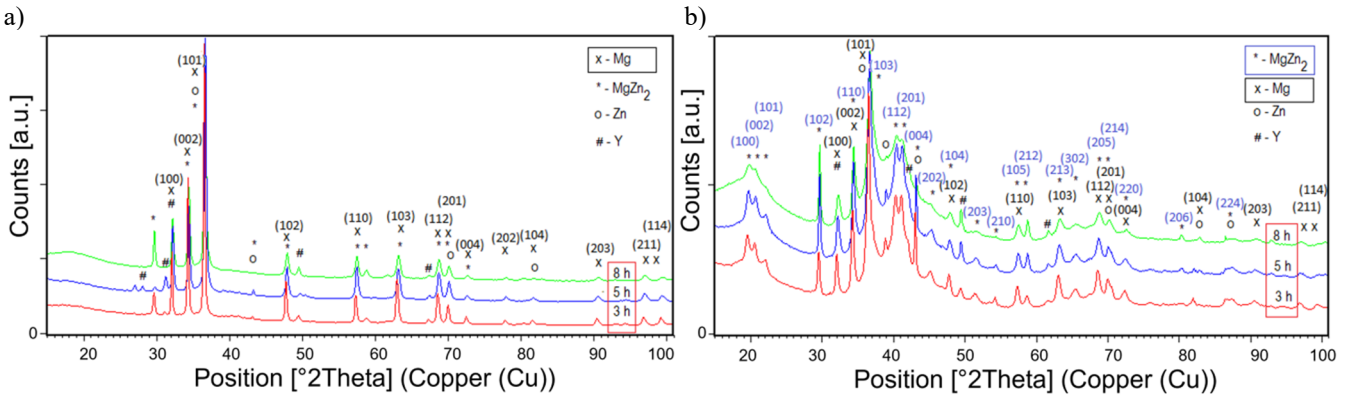

Fig. 1. X-ray diffraction patterns of: a) Mg-2at.%Zn and b) Mg-27at.%Zn samples

Table 2.
Crystallite size and changes of unit cell parameters of solid state solution based on hexagonal Mg – main phase identified for Mg-2at.%Zn sample

Unit cell parameters of Mg(Zn,Y,Ca): a/c, Å				
Sample (milling time)	Theoretical (ICDD PDF4+ card: 04-015-0486)	Refined (RR)	Crystallite size D, Å	Lattice strain η, %
3 h	a = 3.2110 c = 5.2130 Space Group: $P6_3/mmc$ Crystallographic System: hexagonal	3.2086(7)/ 5.2077(9)	744	0.16
5 h		3.2081(9/ 5.2081(4)	362	0.26
8 h		3.2107(6)/ 5.2119(4)	294	0.11

Table 3.
Crystallite size and changes of unit cell parameters of $MgZn_2$ and solid state solution based on hexagonal Mg – main phases identified for Mg-27at.%Zn sample

	Unit cell parameters of $MgZn_2$: a/c, Å				**Unit cell parameters of Mg(Zn,Y,Ca): a/c, Å**			
Sample (milling time)	Theoretical (ICDD PDF4+card: 04-003-2083)	Refined (RR)	Crystallite size D, Å	Lattice strain η, %	Theoretical (ICDD PDF4+ card: 04-015-0486)	Refined (RR)	Crystallite size D, Å	Lattice strain η, %
3 h	a = 5.2230 c = 8.5660 Space Group: $P6_3/mmc$ Crystallographic System: hexagonal	5.2253(2)/ 8.5611(9)	126	0.26	a = 3.2110 c = 5.2130 Space Group: $P6_3/mmc$ Crystallographic System: hexagonal	3.2046(9)/ 5.1984(2)	380	0.42
5 h		5.2461(3)/ 8.6793(3)	120	0.37		3.2021(1)/ 5.1999(2)	330	0.61
8 h		5.3035(8)/ 8.7641(3)	88	1.17		3.1980(9)/ 5.1935(3)	320	0.73

The XRD spectra show the gradual formation of the solid state solution based on hexagonal Mg, $MgZn_2$ phase and the presence of unreacted Zn and Y precursors. Higher Mg content in the Mg-2at.%Zn sample isn't lead to amorphization of the material (Fig. 1a). On the other side, the formation of a solid state solution based on Mg in the amount of 98-99 wt.% is visible in all samples (after 3, 5, 8 hours of milling). The crystallite size of the solid solution gradually decreases with the milling time from 744 to 294 Å (Tab. 2). Slightly lower values of unit cell parameters of the solid solution compared to pure Mg confirms the possibility of dissolving Zn (atomic radius: 1.53 Å) in the hexagonal structure of magnesium (atomic radius: 1.72 Å).

With the increase of milling time, a gradual process of amorphization of the material was observed, especially for the Mg-27at.%Zn sample (Fig. 1b). In this case, the major phase formed in addition to the Mg-based solid solution (30-33 wt.%) is the $MgZn_2$ phase, in an amount of the order of 64-66 wt.%. The rest of the components are unreacted elements: Zn, Y and Ca. The crystallite size of the $MgZn_2$ phase, with increasing milling time, gradually decreases from 126 to 88 Å and for the solid solution, it decreases accordingly from the value of 380 to 320 Å. (Tab. 3). The unit cell parameters of both identified phases slightly differ from the initial values, which may indicate the formation of not only a solid solution based on Mg but also a solid solution based on the $MgZn_2$ phase.

During MA, high energy collisions between the milled powder particles, balls and vial walls generated a great number of structural defects that facilitate diffusion and enabled the formation of solid solutions, intermetallics or amorphous phases. Mechanical alloying caused formation of other phases than during solidification process. During solidification, the LPSO phases Mg-Zn-Y, Mg-Zn-Dy, Mg-Zn-Ho, Mg-Zn-Er and Mg-Zn-Tm [14,15] might be formed. The LPSO phase is nonexistent in as-cast Mg-Zn-Gd and Mg-Zn-Tb ingots but precipitates with soaking at 773 K [15].

3.2. Scanning Electron Microscopy with Energy-Dispersive Spectroscopy

The micrographs of the sample Mg-2at.%Zn milled for 3, 5 and 8 hours are presented in Figure 2. As it can be seen in Figures 2a and 2b, the powder particles vary in size and structure indicating that the alloying process has just begun

and is in progress. This can be observed in the micrographs in Figures 2c,d and 2e,f which represent powders milled for 5 and 8 hours, respectively. After 5 hours, the particles became smaller and more refined. After 8 hours however, they are slightly bigger, which is attributed to the agglomeration of particles. It is visible in Figure 2e, where a big "chunk" is distinctly composed of smaller particles. Moreover in Figure 2f the particles are seen to have jagged edges and are reminiscent of various layers stacked on each other. It is characteristic of the lamellar structure which is created during the repeated cycles of welding and crushing.

Many similarities can be discerned in Figure 3, representing sample Mg-27at.%Zn milled for 3, 5 and 8 hours, respectively. As in case of Figures 2a-b, in Figures 3a-b irregular particles can be seen which are more refined as the process progressed (after 5 hours, Figures 3c-d). In Figures 2 e-f particles with a lamellar structure are visible.

Both samples have been subjected to EDS analysis in order to determine distribution of their chemical composition. The results of the EDS analysis, which was carried out on the surface of a metallographic specimen for Mg-2at.%Zn and Mg-27at.%Zn powder samples after 3, 5 and 8h were

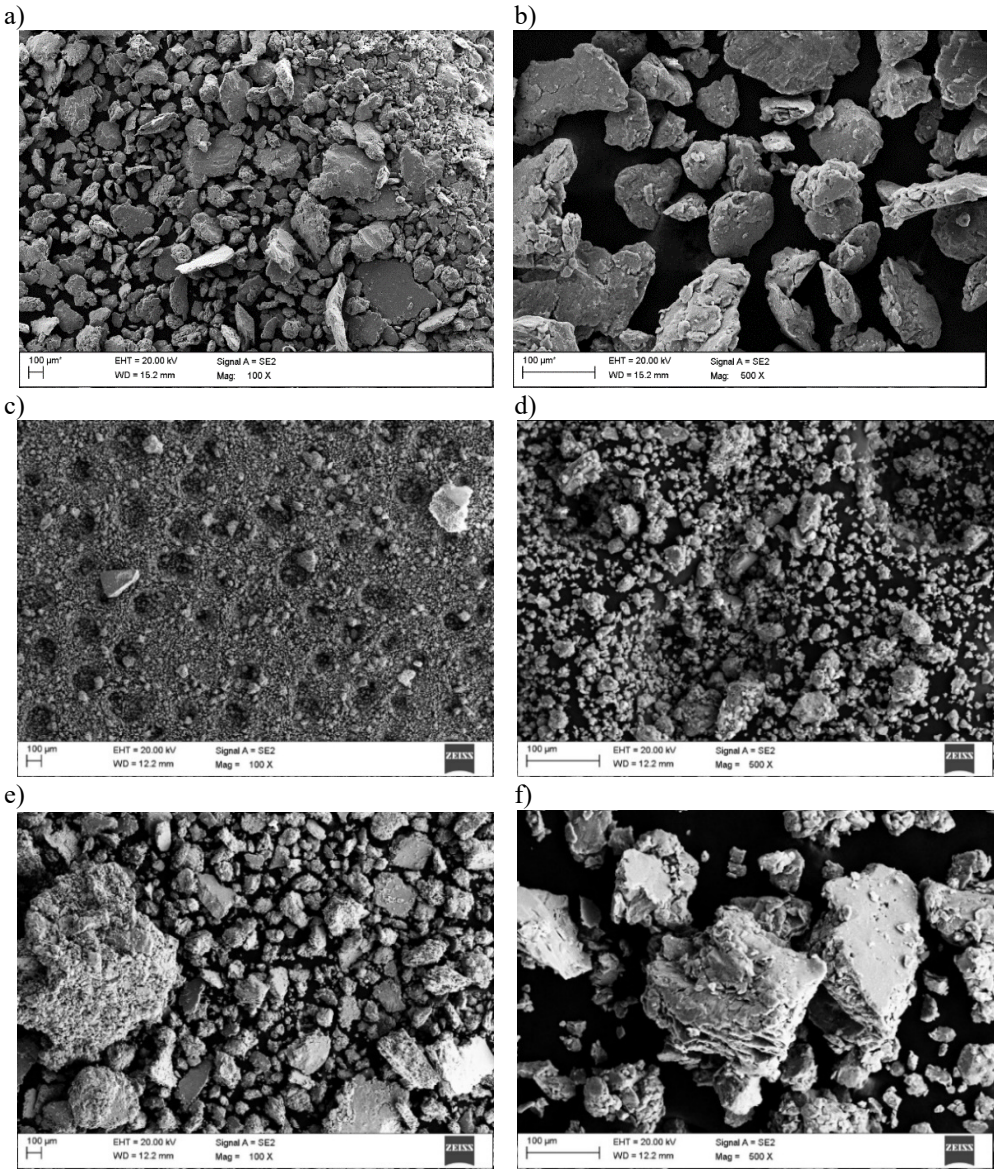

Fig. 2. SEM micrographs of sample Mg-2at.%Zn milled for a, b) 3; c, d) 5 and e, f) 8 hours, respectively. The micrographs presented in left column are at 100x and right at 500x magnitudes

summarized in Tables 4 and 5, respectively. It can be seen in the atomic % chemical composition of both samples (Tabs 4 and 5), that the longer the powder was milled the better the material is mixed and diffused, resulting in a homogeneous dispersion of the elements, thus being close in the margin of error to the assumed chemical composition [32].

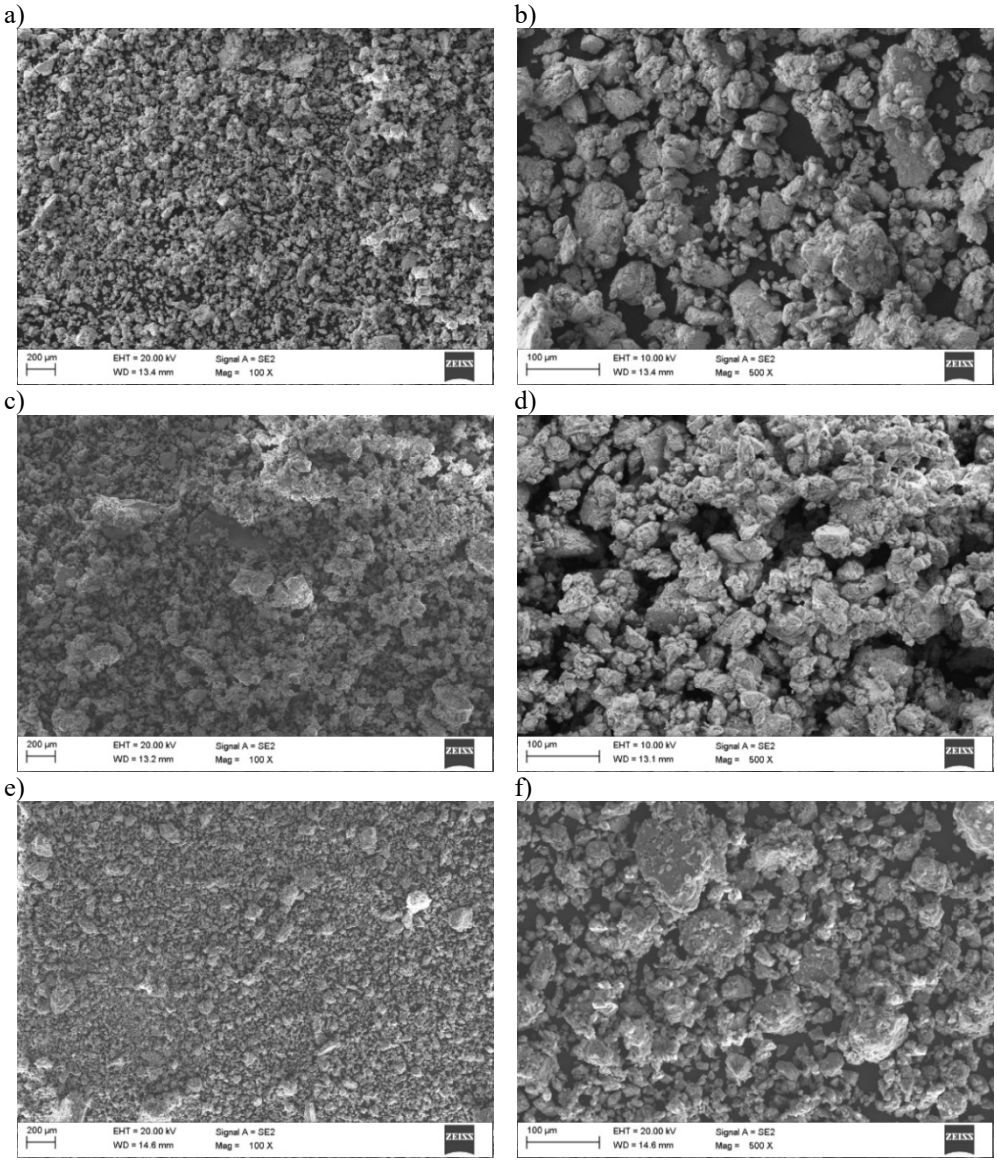

Fig. 3. SEM micrographs of sample Mg-27at.%Zn milled for a, b) 3; c, d) 5 and e, f) 8 hours respectively. The micrographs presented in left column are at 100x and right at 500x magnitudes

Table 4.
EDS (Energy-Dispersive Spectroscopy) results for sample Mg-2at.%Zn milled for 3, 5 and 8 h, respectively. Accuracy of the main elements is about 4 wt. % and minor and trace elements is in a range of 20-50 wt. %

Sample	**wt.%**				**at.%**			
(milling time)	Mg	Zn	Ca	Y	Mg	Zn	Ca	Y
3 h	92.6	4.4	0.3	2.7	97.3	1.7	0.2	0.8
5 h	90.7	5.1	0.8	3.4	96.5	2.0	0.5	1.0
8 h	88.7	5.5	1.0	4.8	95.7	2.2	0.7	1.4

Table 5.
EDS (Energy-Dispersive Spectroscopy) results for sample Mg-27at.%Zn milled for 3, 5 and 8 h, respectively. Accuracy of the main elements is about 4 wt. % and minor and trace elements is in a range of 20-50 wt.%

Sample (milling time)	wt.%				at.%			
	Mg	Zn	Ca	Y	Mg	Zn	Ca	Y
3 h	48.1	48.9	1.0	2.0	71.3	27.0	0.9	0.8
5 h	46.6	49.3	1.3	2.8	70.1	27.6	1.1	1.2
8 h	46.7	48.2	1.3	3.8	70.3	27.0	1.2	1.5

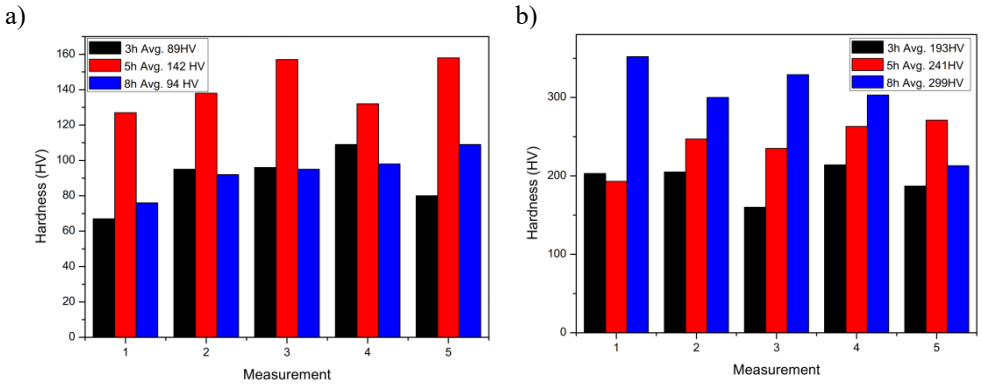

Fig. 4. Microhardness graphical data plots for samples: a) Mg-2at.%Zn and b) Mg-27at.%Zn

3.3. Microhardness and particle size

The hardness value of samples Mg-2at.%Zn increases from 89 to 142 HV after 3 and 5 hours, respectively. After 8 hours hardness drops to 94 HV (shown in Fig. 4a and Tab. 6) as opposed to the samples Mg-27at.%Zn, which the results are presented in Figure 4b and Table 7. This represents an increasing tendency in hardness values with average results of 193, 241 and 299 HV for 3, 5 and 8 hours, respectively.

Table 6.
Microhardness results for sample Mg-2at.%Zn

Sample	Microhardness, HV					Average, HV
	1	2	3	4	5	
3 h	67	95	96	109	80	89
5 h	127	138	157	132	158	142
8 h	76	92	95	98	109	94

Table 7.
Microhardness results for sample Mg-27at.%Zn

Sample	Microhardness, HV					Average, HV
	1	2	3	4	5	
3 h	203	193	352	203	193	193
5 h	205	247	300	205	247	241
8 h	160	235	329	160	235	299

The changes in hardness can be attributed to the powder particles sizes [2,22,33]. In Figures 5 and 6 the particle size volume share and the cumulative distribution of samples Mg-2at.%Zn and Mg-27at.%Zn are shown, respectively. The average particle (D50) of samples Mg-2at.%Zn have values of 162, 53 and 160 µm and samples Mg-27at.%Zn have 182, 36 and 34 µm, respectively. Table 8 summarizes the characteristic values (D10, D50, D90) of particle size for both samples.

Table 8.
Particle size D10, 50 and 90 for investigated samples milled for 3, 5, 8 hours, respectively

Sample	D	Particle size, µm		
		3 h	5 h	8 h
Mg-2at.%Zn	10	53	15	37
	50	162	53	160
	90	389	229	419
Mg-27at.%Zn	10	99	16	13
	50	182	36	34
	90	282	152	186

4. Conclusions

The aim of this work was to produce samples Mg-2at.%Zn and Mg-27at.%Zn by mechanical alloying technique and to study their structure and physical properties. After the mechanical alloying process the particle size analysis for all samples milled by 3, 5 and 8 hours was carried out. The obtained average values were: 163, 53 and 160 µm for Mg-2at.%Zn and 182, 36, 34 µm for samples

Mg-27at.%Zn. The results of the microhardness tests indicate the inversely proportional correlation between particle size and hardness.

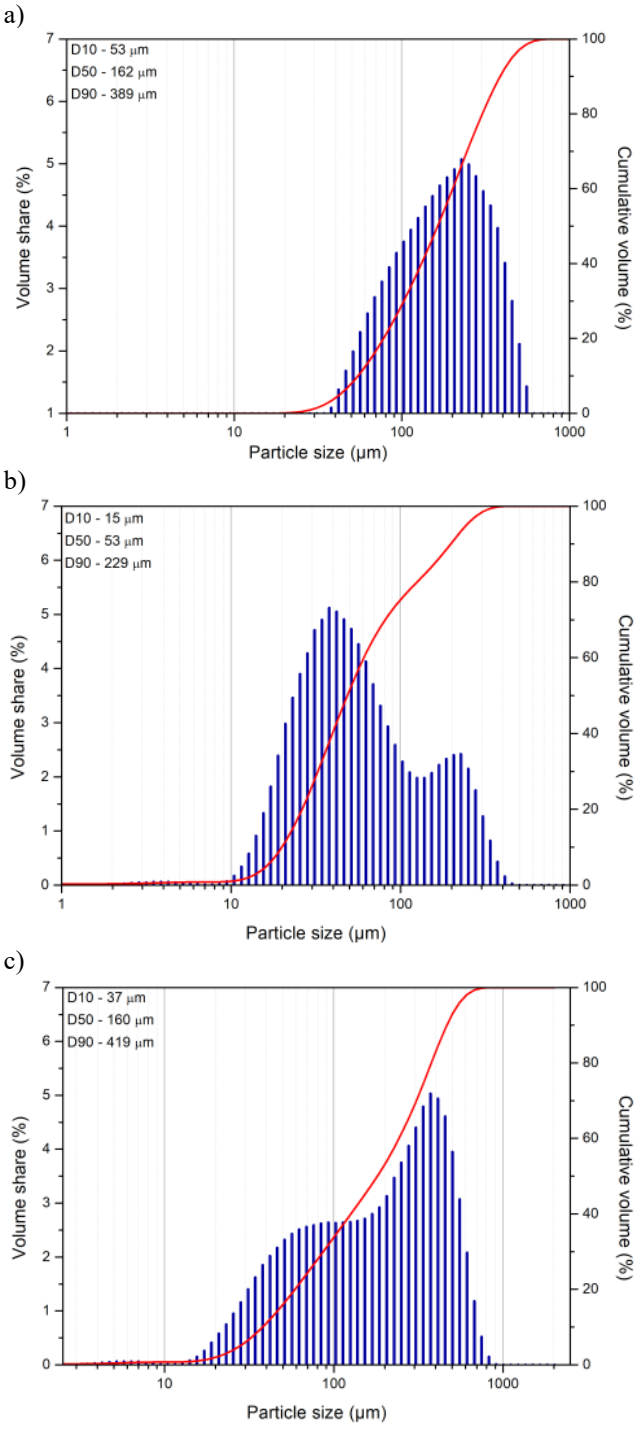

Fig. 5. Particle size volume share (histogram) and their cumulative distribution (curve) for (a-c) sample Mg-2at.%Zn synthesized for 3, 5 and 8 hours, respectively

This correlation is characteristic for mechanical alloying processes. At the time of the milling process the particles are under influence of cyclic welding and fracturing and strong

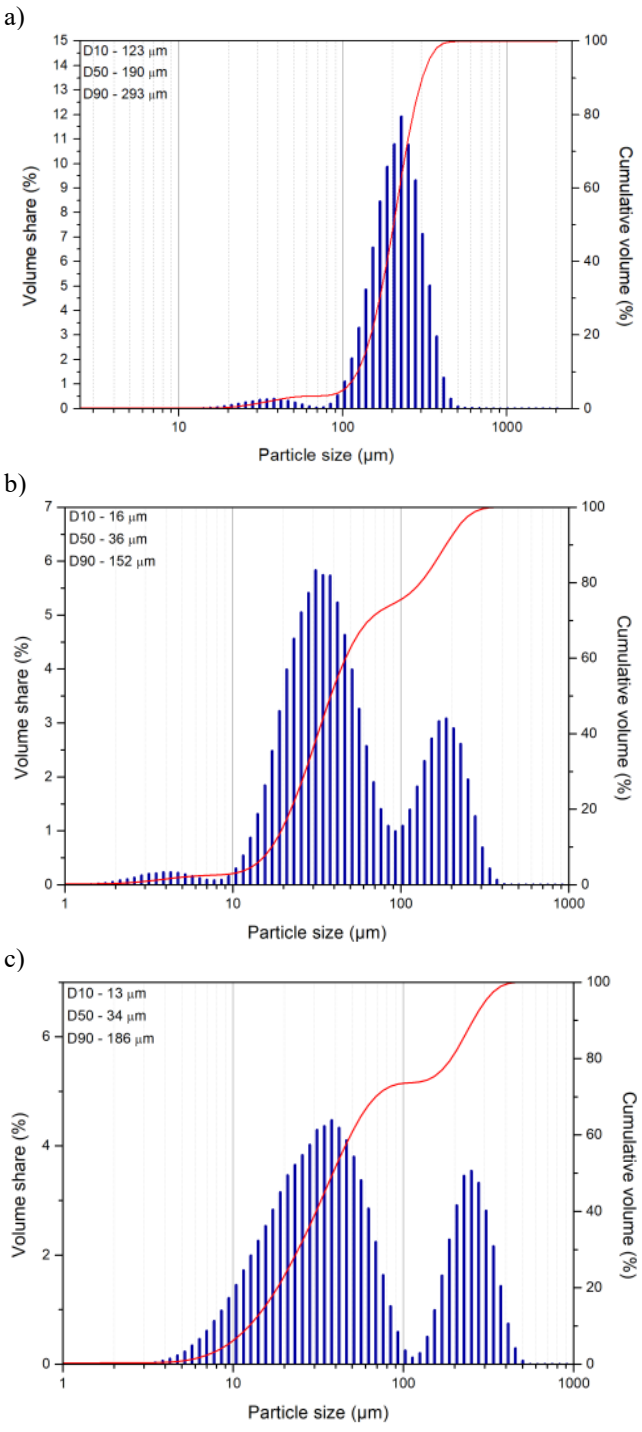

Fig. 6. Particle size volume share (histogram) and their cumulative distribution (curve) for (a-c) sample Mg-27at.%Zn synthesized for 3, 5 and 8 hours, respectively

plastic deformations can be observed. Thus increasing the hardness and decreasing the size. From the difference between the two samples it is closely related to the chemical composition. For sample Mg-27at.%Zn particles decrease in size, Mg-2at.%Zn periodically decreased and increased again.

Therefore, in sample Mg-2at.%Zn after 8 hours milling time the particles started to weld together again. Based on the morphology analysis (SEM) it can be stated that grains of various fineness were obtained.

To conclude:

- The size of the particles depends on both, the time of mechanical alloying and the size of the milling medium (balls).
- The microhardness increases with time for Mg-27at.%Zn, whereas it increases and decreases for samples Mg-2at.%Zn.
- The microhardness is closely related to the particle size, as for sample Mg-2at.%Zn, the particle size increases after 5 hours and decreases after 8 hours. In case of sample Mg-27at.%Zn it increases as the particle size decrease. The same is reflected in the microhardness results.
- Partial amorphization of the milled system is observed only for the sample Mg-27at.%Zn.
- The crystallite size of the Mg-based solid solution of sample Mg-2at.%Zn gradually decreases with the milling time from 744 to 294 Å. For sample Mg-27at.%Zn the crystallite size of the $MgZn_2$ phase gradually decreases from 126 to 88 Å and for the solid solution is changed from 380 to 320 Å.

Acknowledgements

This work was financed by the National Science Center, Poland, grant number 2017/27/B/ST8/02927.

References

[1] M. Gupta N. M. L. Sharon, Magnesium Alloys, and Magnesium Composites, A John Wiley & Sons, Inc.

[2] S. Lesz, J. Kraczla, R. Nowosielski, Structure and compression strength characteristics of the sintered Mg–Zn–Ca–Gd alloy for medical applications, Archievs of Civil and Mechanical Engineering 18/4 (2018) 1288-1299. DOI: https://doi.org/10.1016/j.acme.2018.04.002

[3] L.A. Dobrzański, G.E. Totten, M. Bamberger, Magnesium and Its Alloys: Technology and Applications, CRC Press Taylor & Francis Group Boca Raton, 2020.

[4] D. Ghosh, R. Carnahan, R. Decker, C. Van Schilt, P. Frederick, N. Bradley, Magnesium Alloys and Their Applications, Deutsche Gesellschaft für Metallkunde, 1992.

[5] L.A. Dobrzański, Role of materials design in maintenance engineering in the context of industry 4.0 idea, Journal of Achievements in Materials and Manufacturing Engineering 96/1 (2019) 12-49. DOI:https://doi.org/10.5604/01.3001.0013.7932

[6] L.A. Dobrzański, T. Tański, A. Dobrzańska-Danikiewicz, E. Jonda, M. Bonek, A. Drygała, Structures, properties and development trends of laser-surface-treated hot-work steels, light metal alloys and poly-crystalline silicon, in: J. Lawrence, D.G. Waugh (eds), Laser surface engineering, Processes and applications, Woodhead Publishing Series in Electronic and Optical Materials, Vol. 65, Elsevier, Amsterdam, 2015, 3-32. DOI: https://doi.org/10.1016/B978-1-78242-074-3.00001-5

[7] N. Žaludová, Mg-RE Alloys and Their Applications, WDS'05 Proceedings Contribute Paper, 2005, 8-643.

[8] D. Liu, D. Yang, X. Li, S. Hu, Mechanical properties, corrosion resistance and biocompatibilities of degradable Mg-RE alloys, Journal of Materials Research and Technology 8/1 (2018) 1538-1549. DOI: https://doi.org/10.1016/j.jmrt.2018.08.003

[9] N. Hort, Y. Huang, D. Fechner, M. Störmer, C. Blawert, F. Witte, Magnesium alloys as implant materials – Principles of property design for Mg–RE alloys, Acta Biomaterialia 6/5 (2010) 1714-1725. DOI: https://doi.org/10.1016/j.actbio.2009.09.010

[10] L-N. Zhang, Z-T. Hou, X. Ye, Z-B. Xu, X-L. Bai, P. Shang, The effect of selected alloying element additions on properties of Mg-based alloy as bioimplants, Frontiers in Materials Science 7/3 (2013) 227-236. DOI: https://doi.org/10.1007/s11706-013-0210-z

[11] B. Zhang, A.V. Nagasekhar, X. Tao, Y. Ouyang, C.H. Cáceres, M. Easton, Strengthening by the percolating intergranular eutectic in an HPDC Mg-Ce alloy, Materials Science and Engineering A 599 (2014) 204-211. DOI: https://doi.org/10.1016/j.msea.2014.01.074

[12] Q.A. Li, Q. Zhang, C.Q. Li, Y.G. Wang, Microstructure and mechanical properties of Mg-Y alloys, Materials Research, Trans Tech Publications Ltd, 2011, 5-352. DOI: https://www.scientific.net/AMR.239-242.352

[13] Y. Qu, M. Kang, R. Dong, J. Liu, J. Liu, J. Zhao, Evaluation of a new Mg-Zn-Ca-Y alloy for biomedical application, Journal of Materials Science: Materials in Medicine 26 (2015) 16. DOI: https://doi.org/10.1007/s10856-014-5342-x

[14] D. Egusa, E. Abe, The structure of long period stacking/order Mg-Zn-RE phases with extended non-stoichiometry ranges, Acta Materialia 60/1 (2012) 166-178. DOI: https://doi.org/10.1016/j.actamat.2011.09.030

[15] Y. Kawamura, M. Yamasaki, Formation and mechanical properties of Mg97Zn1RE2 alloys with Long-Period Stacking Ordered structure, Materials

Transactions 48/11 (2007) 2986-2992. DOI: https://doi.org/10.2320/matertrans.MER2007142
[16] X. Gu, Y. Zheng, Y. Cheng, S. Zhong, T. Xi, In vitro corrosion and biocompatibility of binary magnesium alloys, Biomaterials 30/4 (2009) 484-498. DOI: https://doi.org/10.1016/j.biomaterials.2008.10.021
[17] M.K. Datta, D-T. Chou, D. Hong, P. Saha, S.J. Chung, B. Lee, Structure and thermal stability of biodegradable Mg–Zn–Ca based amorphous alloys synthesized by mechanical alloying, Materials Science and Engineering B 176/20 (2011) 1637-1643. DOI: https://doi.org/10.1016/j.mseb.2011.08.008
[18] S. Lesz, M. Kremzer, K. Gołombek, R. Nowosielski, Influence of milling time on amorphization of Mg-Zn-Ca powders synthesized by mechanical alloying technique, Archives of Metallurgy and Materials 63/2 (2018) 839-845. DOI: https://doi.org/10.24425/122413
[19] A. Chrobak, V. Nosenko, G. Haneczok, L. Boichyshyn, M. Karolus, B. Kotur, Influence of rare earth elements on crystallization of $Fe_{82}Nb_2B_{14}RE_2$ (RE=Y, Gd, Tb and Dy) amorphous alloys, Journal of Non-Crystalline Solids 357 (2011) 4-9. DOI: https://doi.org/10.1016/j.jnoncrysol.2010.10.009
[20] L.A. Dobrzański,The significance of the nanostructural components on the properties of the nanoengineering materials, Journal of Achievements in Materials and Manufacturing Engineering 88/2 (2018) 55-85. DOI: https://doi.org/10.5604/01.3001.0012.6150
[21] L.A. Dobrzański, L.B. Dobrzański, A.D. Dobrzańska-Danikiewicz, Additive and hybrid technologies for products manufacturing using powders of metals, their alloys and ceramics, Archives of Materials Science and Engineering 102/2 (2020) 59-85. DOI: https://doi.org/10.5604/01.3001.0014.1525
[22] M. Jurczyk, Mechanical alloying, Poznan University of Technology Press, Poznań, 2003 (in Polish).
[23] C. Suryanarayana, Mechanical alloying and milling, Progress in Material Science 46/1-2 (2001) 1-184. DOI: https://doi.org/10.1016/S0079-6425(99)00010-9
[24] J.F. Wang, Y.Y Wei, S.F. Guo, S. Huang, X.E. Zhou, F.S. Pan, The Y-doped MgZnCa alloys with ultrahigh specific strength and good corrosion resistance in simulated body fluid, Materials Letters 81 (2012) 112-114. DOI: https://doi.org/10.1016/j.matlet.2012.04.130
[25] A.T. Olanipekun, N.B. Maledi, P.M. Mashinini, The synergy between powder metallurgy processes and welding of metallic alloy, Powder Metallurgy 63/4 (2020) 254-267. DOI: https://doi.org/10.1080/00325899.2020.1807712
[26] Y. Han, D. Zou, Z. Chen, G. Fan, W. Zhang, Investigation on hot deformation behavior of 00Cr23Ni4N duplex stainless steel under medium–high strain rates, Materials Characterization 62/2 (2011) 198-203. DOI: https://doi.org/10.1016/j.matchar.2010.11.013
[27] J.M. Dutkiewicz, W. Maziarz, T. Czeppe, L. Lityńska, W.K. Nowacki, S.P. Gadaj, Powder metallurgy technology of NiTi shape memory alloy, European Physical Journal Special Topics 158 (2008) 59-65. DOI: https://doi.org/10.1140/epjst/e2008-00654-6
[28] O.D. Neikov, V.G. Gopienko, Production of Magnesium and Magnesium Alloy Powders, Handbook of Non-Ferrous Metal Powders, Elsevier, 2019, 533-547. DOI: https://doi.org/10.1016/B978-0-08-100543-9.00017-8
[29] L.A. Dobrzański, L.B. Dobrzański, A.D. Dobrzańska-Danikiewicz, Overview of conventional technologies using the powders of metals, their alloys and ceramics in Industry 4.0 stage, Journal of Achievements in Materials and Manufacturing Engineering 98/2 (2020) 56-85. DOI: https://doi.org/10.5604/ 01.3001.0014.1481
[30] L.A. Dobrzański, L.B. Dobrzański, A.D. Dobrzańska-Danikiewicz, M. Kraszewska, Manufacturing powders of metals, their alloys and ceramics and the importance of conventional and additive technologies for products manufacturing in Industry 4.0 stage, Archives of Materials Science and Engineering 102/1 (2020) 13-41. DOI: https://doi.org/10.5604/ 01.3001.0014.1452
[31] J.S. Benjamin, T.E. Volin, The mechanism of mechanical alloying, Metallurgical Transactions 5 (1974) 1929-1934. DOI: https://doi.org/10.1007/BF02644161
[32] M. Karolus, J. Panek, Nanostructured Ni-Ti alloys obtained by mechanical synthesis and heat treatment, Journal of Alloys and Compounds 658 (2016) 709-715. DOI: http://doi.org/10.1016/j.jallcom.2015.10.286
[33] J.B. Fogagnolo, F. Velasco, M. Robert, J. Torralba, Effect of mechanical alloying on the morphology, microstructure and properties of aluminium matrix composite powders, Materials Science and Engineering A 342/1-2 (2003) 131-143. DOI: https://doi.org/10.1016/S0921-5093(02)00246-0
[34] M. Jurczyk, Bionanomaterials for Dental Applications, Pan Stanford Publishing, 2012.